BIOCHEMISTRY
including biophysical chemistry & molecular biology

Article

pubs.acs.org/biochemistry

Inactivation Mechanism of Glycerol Dehydration by Diol Dehydratase from Combined Quantum Mechanical/Molecular Mechanical Calculations

Kazuki Doitomi,[†] Takashi Kamachi,[†] Tetsuo Toraya,[‡] and Kazunari Yoshizawa*[,†]

[†]Institute for Materials Chemistry and Engineering and International Research Center for Molecular Systems, Kyushu University, Fukuoka 819-0395, Japan

[‡]Graduate School of Natural Science and Technology, Okayama University, Okayama 700-8530, Japan

Supporting Information

ABSTRACT: Inactivation of diol dehydratase during the glycerol dehydration reaction is studied on the basis of quantum mechanical/molecular mechanical calculations. Glycerol is not a chiral compound but contains a prochiral carbon atom. Once it is bound to the active site, the enzyme adopts two binding conformations. One is predominantly responsible for the product-forming reaction (G_R conformation), and the other primarily contributes to inactivation (G_S conformation). Reactant radical is converted into a product and byproduct in the product-forming reaction and inactivation, respectively. The OH group migrates from C2 to C1 in the product-forming reaction, whereas the transfer of a hydrogen from the 3-OH group of glycerol to C1 takes place during the inactivation. The activation barrier of the hydrogen transfer does not depend on the substrate-binding conformation. On the other hand, the activation barrier of OH group migration is sensitive to conformation and is 4.5 kcal/mol lower in the G_R conformation than in the G_S conformation. In the OH group migration, Glu170 plays a critical role in stabilizing the reactant radical in the G_S conformation. Moreover, the hydrogen bonding interaction between Ser301 and the 3-OH group of glycerol lowers the activation barrier in G_R-TS2. As a result, the difference in energy between the hydrogen transfer and the OH group migration is reduced in the G_S conformation, which shows that the inactivation is favored in the G_S conformation.

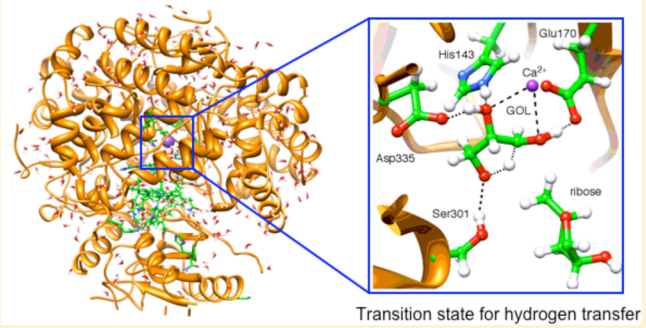

Transition state for hydrogen transfer

Diol dehydratase (DD) is an adenosylcobalamin (AdoCbl)-dependent enzyme that catalyzes the conversion of 1,2-propanediol (PDO), glycerol (GOL), and 1,2-ethanediol to the corresponding aldehydes.[1−4] Figure 1 depicts the generally accepted minimal mechanism for the reactions catalyzed by DD.[5−18] The enzymatic reactions are initiated by the homolytic cleavage of the Co−C bond of the enzyme-bound cofactor. The produced adenosyl radical abstracts a hydrogen atom from C1 to form the reactant (substrate) radical, and then the OH group migrates to C1, leading to the formation of the product radical. The resultant product radical reabstracts a hydrogen atom from 5′-deoxyadenosine, which leads to the formation of the 1,1-diol and the regeneration of the adenosyl radical.

Crystal structure analyses[19−22] of the DD complex with adeninylpentylcobalamin and PDO have provided an important hint for understanding the reaction at the molecular level. There is a metal ion in the inner cavity of the active site. The metal ion is coordinated by five oxygen atoms that originated from the side chains of Gln141, Glu170, Glu221, and Gln296 and the carbonyl group of Ser362 (residue numbers in the α-subunit). The sixth and seventh coordination positions are occupied by two hydroxyl groups of PDO. Recently, we proposed from quantum mechanical/molecular mechanical (QM/MM) calculations that the central metal is a calcium ion.[23] This assumption was experimentally confirmed by Toraya and co-workers. They reported that the Ca-derived DD is catalytically inactive, which indicates that DD is a K^+-dependent Ca-metalloenzyme.[24] Very recently, we evaluated from QM/MM computations the catalytic role of the Ca ion in the hydrogen atom abstraction and the OH group migration processes catalyzed by DD.[25] The Ca ion has strong electron withdrawing power, which contributes to the reduction of the activation barrier for OH group migration.

DD is subject to "suicide inactivation" in the catalysis of substrate and product analogues, GOL,[26−28] glycolaldehyde,[29] and 2-chloroacetaldehyde.[30] In EPR experiments, Frey and Reed identified byproducts derived from both glycolaldehyde and 2-chloroacetaldehyde as *cis*-ethanesemidione,[31,32] which was recently supported by theoretical calculations.[33,34] The byproduct of glycerol inactivation has not been identified, but Bachovchin and co-workers provided important clues. GOL is

Received: April 16, 2012
Revised: October 23, 2012
Published: October 25, 2012

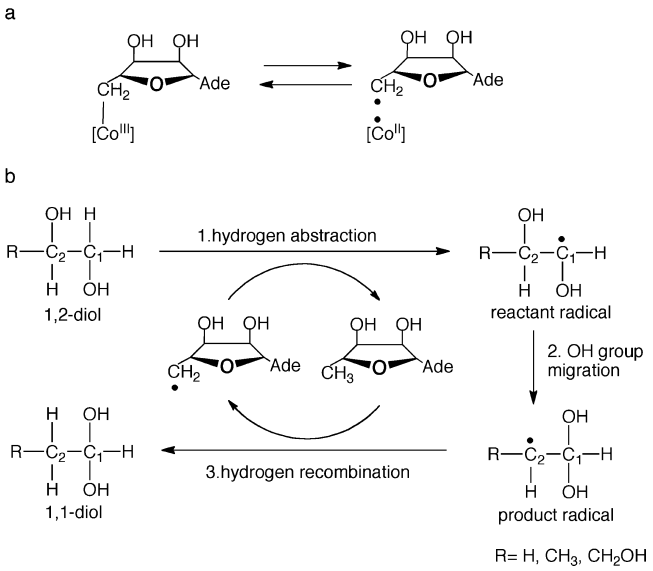

Figure 1. Minimal mechanism of the diol dehydratase reaction. (a) Homolysis of the Co−C bond in AdoCbl. (b) Adenosyl radical-catalyzed enzymatic rearrangements.

not a chiral compound, but once it is bound to the active site, the enzyme can distinguish its two binding conformations. They defined the two binding conformations of GOL as follows: "G_S" represents glycerol bound to the enzyme with the *pro-S*-CH_2OH group at the site involved in hydrogen abstraction, while "G_R" represents the corresponding enzyme−GOL complex with the *pro-R*-CH_2OH group so oriented. From the kinetic study of DD inactivation with various deuterated glycerols, they concluded that GOL bound in the G_R conformation is mainly responsible for the product-forming reaction, while the GOL bound in the G_S conformation primarily contributes to the inactivation.[27] Very recently, the crystal structure analysis of the DD complex with cyanocobalamin and GOL indicated that GOL is bound in the G_S conformation.[35] The O3−Oε (Gln336) and O3−Oγ (Ser301) bond lengths are 3.01 and 2.54 Å, respectively, as shown in Figure 2. As judged from the directions, the O3 atom would be hydrogen bonded to Ser301, but not to Gln336.

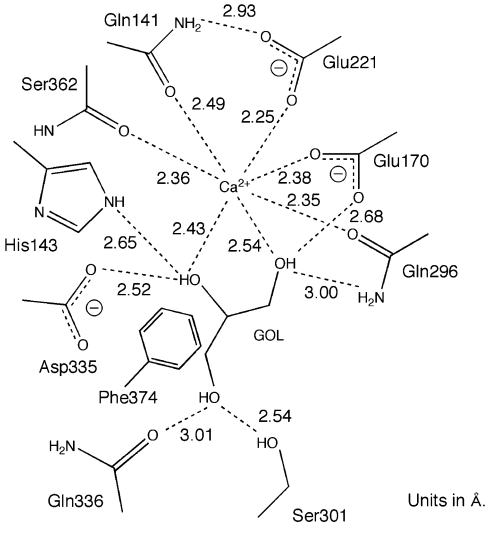

Figure 2. X-ray crystal structure of DD in complex with GOL.

Toraya and co-workers proposed that the hydrogen bond between O3 and Oγ increases the barrier height of OH group migration from the G_S conformation, whereas it does not significantly affect that from the G_R conformation. As a result, side reactions leading to the inactivation would take place at a higher probability from the G_S conformation. This work seeks to provide insight into the mechanism of inactivation from a computational analysis of reaction profiles for the dehydration of GOL in the G_S and G_R conformations.

METHOD OF CALCULATION

System Setup. We built a QM/MM model of DD on the basis of the crystal structure of DD in complex with cyanocobalamin and GOL (PDB entry 3AUJ). The protonation states of titratable residues at pH 8 were estimated by the generalized Born method.[36−38] The protonation states were cross-checked with another pK_a prediction program, PROPKA.[39,40] To reduce the computational cost for QM/MM calculations, the size of the entire system has to be reduced: the constructed enzyme model includes ligands, water molecules, and all amino acids that have atoms within 30 Å of any atom of the substrate, resulting in 12254 atoms in total. The dangling bonds at the boundary are capped with hydrogen atoms. The crystal structure does not include adenosine, which acts as a radical source in the reaction. To predict a favorable adenosine binding structure, we superimposed the two enzymes: the DD−AdoCbl complex, which was used in our previous calculation, and PDB entry 3AUJ. In this study, we decided to replace HOH90 with a K ion, as observed in the crystal structure of the diol dehydratase−adeninylpentylcobalamin complex (PDB entry 1EEX), and deleted five water molecules (HOH1−HOH4 and HOH6) that overlapped with adenosine. The cation is necessary to stabilize the Ado moiety in the enzyme pocket.

The system was heated and equilibrated at the CHARMm[41−43] level of theory in three steps: (i) steepest descent optimization of the system to eliminate bad contacts (rms gradient of <0.1 kcal mol^{-1} $Å^{-1}$), (ii) molecular dynamics (MD) for 15 ps with heating from 50 to 300 K with the leapfrog Verlet integrator, and (iii) equilibration for 400 ps at 300 K with a time step of 1 fs. During the initial optimization and the classical MD simulation, the coordinates of the QM region atoms defined in the following section and of heavy atoms >20 Å from any atom of the substrate were kept fixed at the X-ray coordinates to preserve the X-ray structure. The coordinates of the corrin ring were also fixed at the X-ray crystal structure. We used CHARMm parameters for cobalamin reported in our previous papers.[23,25] The SHAKE algorithm[44] was used to constrain bonds involving hydrogen atoms. Finally, the system was minimized with the adopted basis Newton−Raphson (ABNR)[45] algorithm for 5000 steps. All calculations were conducted with Discovery Studio 2.0.[46]

QM/MM Calculations. An initial geometry for QM/MM calculations was obtained in the setup phase. The QM region contains GOL, the ribose moiety of the adenosyl radical, calcium ion, the side chains of Gln141, His143, Glu170, Glu221, Gln296, Ser301, Asp335, Gln336, and Phe374, and the carbonyl group of Ser362 (Figure 2). ChemShell version 3.2[47] was used to perform QM/MM calculations by integrating TURBOMOLE[48] for QM calculations and the DL-POLY[49] for MM calculations. Link atoms were introduced to saturate the valence of the QM boundary atoms with the L2 scheme,[50] where the linking H atom does not interact with the MM atoms

dx.doi.org/10.1021/bi300488u | *Biochemistry* 2012, 51, 9202−9210

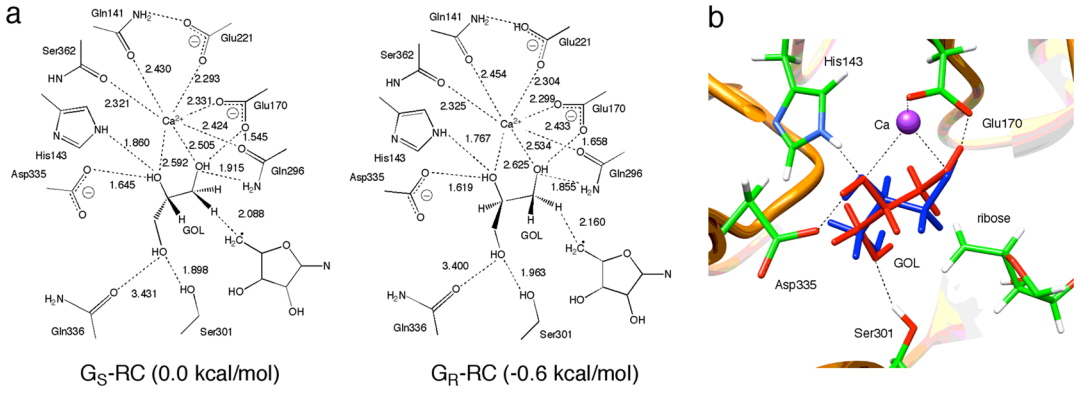

Figure 3. (a) QM/MM-optimized structure of the substrate-binding site with G_S and G_R (distances in angstroms). Relative energies are measured from the G_S-RC conformation. (b) Overlay of DD with GOL in G_S-RC (red) and G_R-RC (blue).

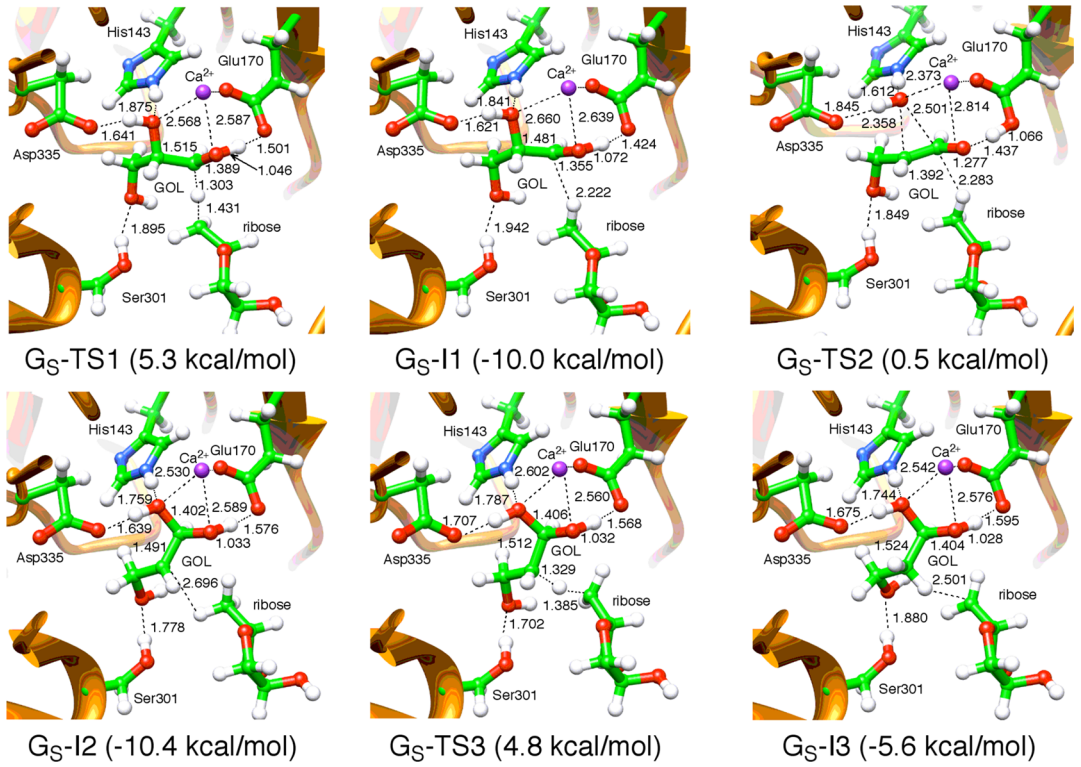

Figure 4. Optimized geometries of intermediates and transition states for hydrogen abstraction, OH group migration, and hydrogen recombination in the G_S conformation (distances in angstroms). Relative energies are measured from G_S-RC shown in Figure 3a.

of the adjacent neutral charge group by deletion of MM point charges on all atoms in the neutral group in the QM part of the QM/MM calculations. For the QM calculations, the B3LYP functional[51−53] was used in combination with the SV(P)[54] basis set for geometry optimization. Single-point calculations of the optimized structures were computed with the TZVP[55] basis set. The CHARMm force field was used for the MM region. A standard electronic embedding scheme[56] was chosen; the fixed MM atomic charges were included in the one-electron Hamiltonian of the QM calculations, and the QM/MM electrostatic interactions were evaluated from the QM electrostatic potential and the MM atomic charges. The complete nonbonding MM and QM/MM interactions were calculated without employing any cutoff. We defined a region with 1160 atoms to be fully optimized by including all residues that have atoms within 10 Å of any atom of the substrate, while we kept the remaining atoms fixed. The coordinates of the corrin ring were also fixed at the X-ray structure. It is unlikely that the calculated energies are significantly affected by the fixations. The distance between the metal ion and the Co atom of the corrin ring is 11.5 Å in the X-ray structure, and therefore, cobalamin acts solely as a spectator in hydrogen transfer and OH group migration.[57] Geometry optimizations were performed with the HDLC optimizer[58] in ChemShell. To confirm that there are no artificial effects on the relative energies due to different local minima in the MM region, we conducted a series of optimizations from a transition state iterating back and forth between all stationary points until the convergence of QM/MM energies (<1 kcal/mol). The QM/MM energies are also summarized in the Supporting Information. Vibrational frequencies were computed for all stationary points to confirm that each optimized geometry corresponds to a local minimum that has no imaginary frequency or to a saddle point that has only one imaginary frequency. Zero-point vibrational energy

dx.doi.org/10.1021/bi300488u | *Biochemistry* 2012, 51, 9202−9210

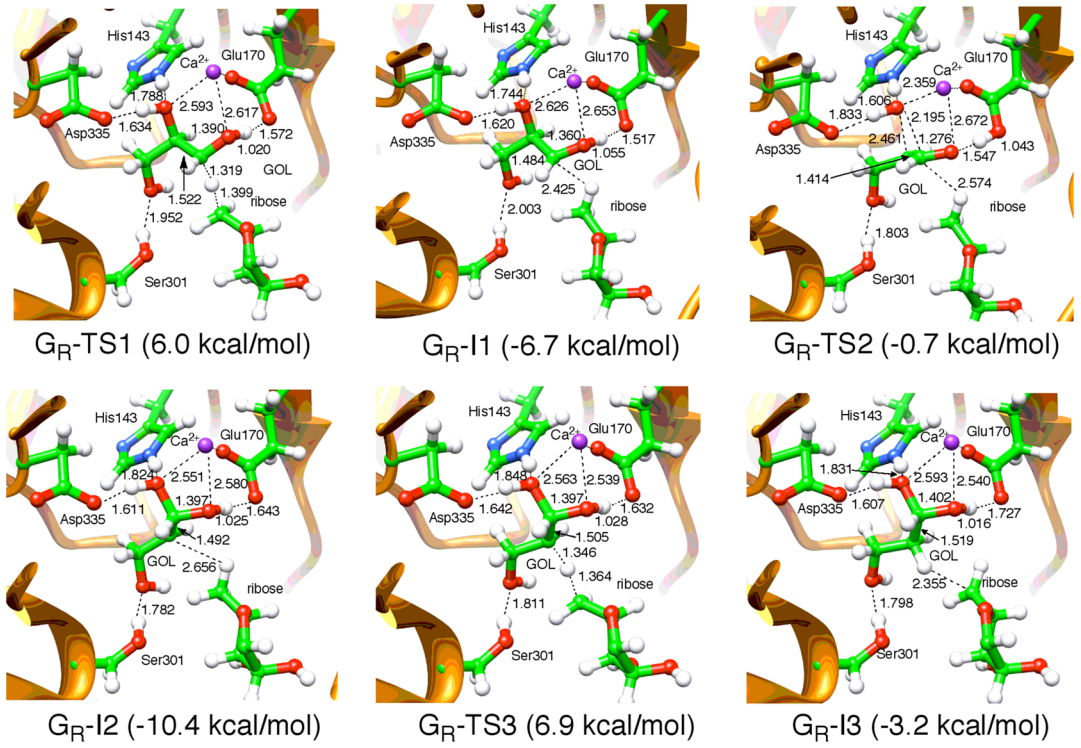

Figure 5. Optimized geometries of intermediates and transition states for hydrogen abstraction, OH group migration, and hydrogen recombination in the G_R conformation (distances in angstroms). Relative energies are measured from G_S-RC shown in Figure 3a.

corrections were taken into account in calculating the total energies of the reaction species.

RESULTS AND DISCUSSION

Structures of the G_S and G_R Conformations. Figure 3a shows the substrate-binding site in QM/MM-optimized structures of the reactant complex (RC) with GOL in the G_S and G_R conformations (G_S-RC and G_R-RC, respectively). The two conformations are bound in a symmetrical mode as mirror images with respect to the plane including Ca, O1, and O2, as shown in Figure 3b. The amino acid residues that form hydrogen bonds with GOL are essentially the same in both conformations. That is, O1 is hydrogen-bonded to Glu170 and Gln296, O2 to Asp335 and His143, and O3 to Ser301. The metal−oxygen bond lengths are almost identical between both conformations except those of the O1−Ca and O2−Ca bonds. The O1−Ca and O2−Ca bond lengths are 0.033 and 0.029 Å longer in G_R-RC than in G_S-RC, respectively, which indicates that GOL is more strongly bonded to the Ca ion in G_S-RC. We also found the difference in hydrogen bonding distances between GOL and the active site amino acid residues in the two conformations. An important factor in controlling the conformation of GOL is hydrogen bonding interaction with amino acid residues in the active site. The distances between Gln296 and GOL, Asp335 and GOL, and His143 and GOL are 0.060, 0.036, and 0.093 Å shorter, respectively, in G_R-RC than in G_S-RC, but the distance between Glu170 and GOL is 0.113 Å longer in G_R-RC than in G_S-RC. Moreover, the conformational difference affects the hydrogen bonding distance between Ser301 and the 3-OH group, which is 0.065 Å longer in G_R-RC than in G_S-RC.

We considered another possible substrate binding form, in which the 3-OH group acts as a donor of a hydrogen bond to Gln336 and as an acceptor of a hydrogen bond from Ser301. This structure is 1.7 kcal/mol more unstable than the G_S conformation, which indicates that the 3-OH group is hydrogen bonded to Ser301, but not to Gln336, as observed in the crystal structure.[35]

Hydrogen Abstraction. Figures 4 and 5 show optimized geometries of reactant radical (I1), product radical (I2), and 1,1,3-propanetriol (I3) intermediates, and transition states for hydrogen abstraction (TS1), OH group migration (TS2), and hydrogen recombination (TS3) steps in the G_S and G_R conformations, respectively. We present only the Ca ion, the substrate, the ribose moiety, His143, Glu170, Ser301, and Asp335 for the sake of clarity. The adenosyl radical abstracts the *pro-S* hydrogen and *pro-R* hydrogen atom from GOL in the G_S and G_R conformations, respectively. The activation barrier of 6.6 kcal/mol for TS1 in G_R-TS1 is 1.3 kcal/mol higher than the corresponding barrier in G_S-TS1 because of the longer distance between the adenosyl radical and the abstracted hydrogen atom; the H−C5′ distance is 2.088 and 2.160 Å in G_S-RC and G_R-RC, respectively. In I1, several structural changes were observed upon comparison with RC. In particular, the O (Glu170)−H bond distance decreases by 0.121 and 0.141 Å in G_S-I1 and G_R-I1, respectively. This intermediate is an α-hydroxy radical species, which is up to 10^5 times more acidic than the corresponding alcohols.[59−61] The C1−O1 bond length decreases from 1.415 (1.417) Å in RC to 1.355 (1.360) Å in G_S-I1 (G_R-I1). This geometrical change is due to the resonance structure possessing an O-centered radical and the concomitant C1−O1 double bond, as proposed in our previous study.[25]

OH Group Migration. Golding and Radom proposed that the barrier height of the OH group migration step is lowered through the partial protonation of the migrating OH group and the partial deprotonation of the spectator OH group in the PDO dehydration reaction using simple model calcula-

dx.doi.org/10.1021/bi300488u | *Biochemistry* 2012, 51, 9202−9210

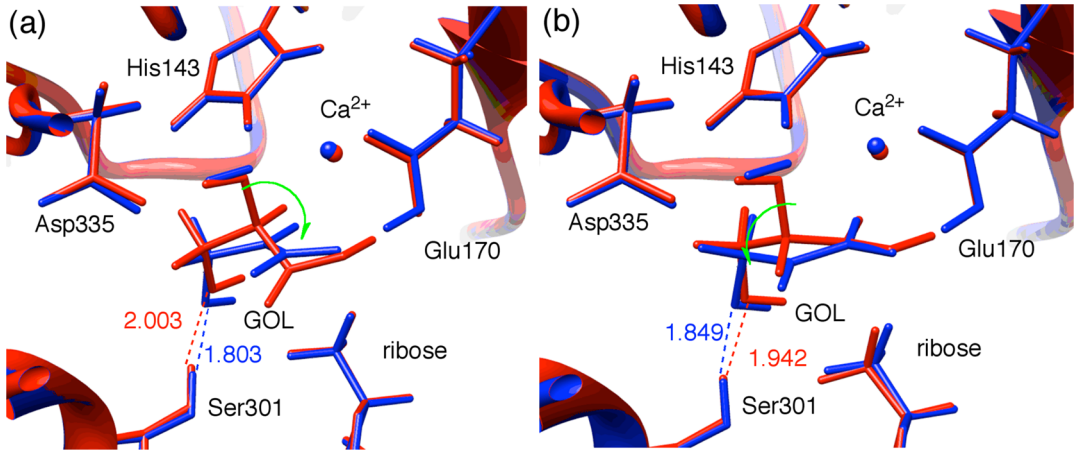

Figure 6. Superimposition of the QM/MM-optimized structures of I1 (red) and TS2 (blue) in the (a) G_R and (b) G_S conformations. The green arrows indicate the direction of OH group migration. The key distances are given in angstroms.

Table 1. QM/MM, QM, and QM(gas) Energies (kilocalories per mole) Measured for G_S-RC

	RC	TS1	I1	TS2	I2	TS3	I3
				G_S			
QM/MM[a]	0.0	7.5	−9.9	2.5	−10.4	7.3	−5.4
QM[b]	0.0	8.1	−10.6	0.2	−11.7	4.9	−7.0
QM(gas)[c]	0.0	10.0	−9.6	4.1	−9.6	10.6	−6.7
				G_R			
QM/MM[a]	−0.9	8.5	−6.5	0.7	−10.5	9.2	−3.9
QM[b]	−0.5	9.7	−7.9	−1.8	−11.3	8.5	−6.1
QM(gas)[c]	−1.3	10.8	−6.5	3.4	−8.2	13.2	−3.6

[a]QM/MM energies do not include zero-point vibrational energy corrections. [b]QM energies of the QM/MM-optimized structure with MM point charges. [c]QM energies of the QM/MM-optimized structure without MM point charges.

tions.[62−66] We previously reported that OH group migration proceeds in a concerted manner via a transition state with a triangle structure and that the activation barrier for OH group migration is lowered by the deprotonation of the spectator OH group by Glu170 in the PDO dehydration reaction.[25,67,68] OH group migration in GOL dehydration occurs in a manner similar to that in PDO dehydration. The transition state of this step also has a triangle structure; the C1−C2, C1−O2, and C2−O2 bond lengths are 1.392 (1.414), 2.501 (2.195), and 2.358 (2.461) Å, respectively, in G_S-TS2 (G_R-TS2). In the transition state, the COO^- group of Glu170 temporarily accepts a proton from the 1-OH group; the O1−H and O (Glu170)−H bond lengths are 1.437 (1.547) and 1.066 (1.043) Å in G_S-TS2 (G_R-TS2), respectively. The calculated bond orders for the O1−H and O (Glu170)−H bonds are 0.27 (0.20) and 0.68 (0.73) in G_S-TS2 (G_R-TS2), respectively, which indicate that Glu170 more effectively activates the 1-OH group in G_R-TS2. The C1−O1 and C1−C2 bond lengths are slightly shorter than the typical bond lengths, and the C1−O1 and C1−C2 bond orders are 1.32 (1.37) and 1.29 (1.14) in G_S-TS2 (G_R-TS2), respectively. These results indicate that the transition states have resonance structures to stabilize the transition state, as proposed in the PDO dehydration reaction.[25] The activation barrier of TS2 was calculated to be 10.5 and 6.0 kcal/mol in the G_S and G_R conformations, respectively. Why is the barrier 4.5 kcal/mol higher in the G_S conformation? QM/MM computations revealed three factors that affect the barrier of TS2. First, Ser301 controls structural changes in GOL accompanied by OH group migration with a hydrogen bond to the 3-OH group as proposed by Toraya and co-workers.[35] When the OH group migrates from C2 to C1 in the G_R conformation, the C−C−C backbone rotates clockwise around the axis connecting Ca and the center of the O1−O2 line. In the G_R conformation, the length of the hydrogen bond between Ser301 and GOL is shortened by 0.200 Å from 2.003 Å in I1 to 1.803 Å in TS2 (Figure 6a). In contrast, in the G_S conformation, the C−C−C backbone rotates anticlockwise, the hydrogen bonding distance being shortened by only 0.093 Å (Figure 6b).

Second, the reactant radical is significantly stabilized by Glu170 in the G_S conformation. G_S-I1 lies 3.3 kcal/mol below G_R-I1, which is mainly due to the QM energy difference (Table 1). To estimate the importance of the key residues (His143, Glu170, Ser301, and the Ca^{2+}) on the energy difference, we extracted the QM region except the residues from the QM/MM-optimized structure to perform single-point calculations with the MM point charges. The energy differences are 2.7, 3.6, 2.9, and −0.7 kcal/mol in the absence of His143, Ser301, Ca^{2+}, and Glu170, respectively, which shows that Glu170 plays a major role in stabilizing G_S-I1. This is because the reactant radical is tightly hydrogen bonded to Glu170 in the G_S conformation. The hydrogen bond lengths are 1.424 and 1.517 Å in G_S-I1 and G_R-I1, respectively.

Third, the protein environment has a significant influence on the energy barrier of TS2, as shown in Table 1. The activation barrier of G_S-TS2 (G_R-TS2) is reduced by 2.9 (3.8) kcal/mol due to the MM point charges [see the energy difference between QM and QM(gas)]. The amino acids that have strong electrostatic effects on the activation energy are listed in Table 2. The major electrostatic effect comes from Arg193, Ser202,

dx.doi.org/10.1021/bi300488u | Biochemistry 2012, 51, 9202−9210

Table 2. Electrostatic Stabilization Energies (kilocalories per mole) between the QM and MM Regions for G_S-TS2 Relative to G_S-I1 and for G_R-TS2 Relative to G_R-I1[a]

G_S-TS2		G_R-TS2	
Arg193	−3.4	Arg193	−4.8
Ser202	2.4	Ser202	3.1
Arg348	−2.1	Arg348	−2.3
Thr171	−1.1	Ser224	−1.6
Glu204	−1.0	Ser303	−1.6
HOH1213	−0.9	Thr171	−1.2
Ser333	−0.9	Glu204	−1.2
Asp383	0.9	His216	0.9
His216	0.8	Gln200	0.9
Arg345	−0.8	Arg344	−0.9

[a]The top 10 residues are listed.

and Arg348 (Figure 7).[69,70] In TS2, GOL is negatively charged because of the shift of the proton from GOL to Glu170. Thus,

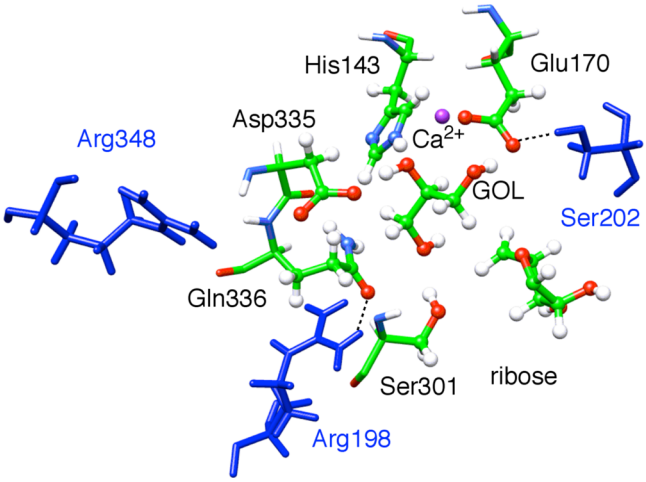

Figure 7. Key residues (blue) in the MM region that reduce the barrier for TS2. QM atoms are shown as balls and sticks, and MM atoms are shown as sticks.

the positively charged residues (Arg193 and Arg348) stabilize the negatively charged GOL. On the other hand, a hydrogen bond between Glu170 and the OH group of Ser202 is weakened in TS2 because Glu170 is neutralized by the protonation.

Inactivation Mechanism. We[25,67,68] and Radom and co-workers[33,34,71−73] reported that the activation barrier for the hydrogen recombination reaction is slightly higher than that for the initial abstraction reaction and proposed that hydrogen recombination is the rate-limiting step. Hydrogen recombination (TS3) is also the most energy-demanding step in the GOL dehydration reaction; the activation barriers are calculated to be 15.2 and 17.3 kcal/mol in G_S-TS3 and G_R-TS3, respectively. This is consistent with the experimental findings that the deuterium kinetic isotopic effect on the product-forming reaction is 8.0.[27]

Inactivation would take place prior to hydrogen recombination. We assumed that inactivation begins with an intramolecular transfer of hydrogen from the 3-OH group of GOL to the C1 radical with the formation of an O-centered radical (I_{inact}), as shown in Scheme 1. Figure 8 shows optimized

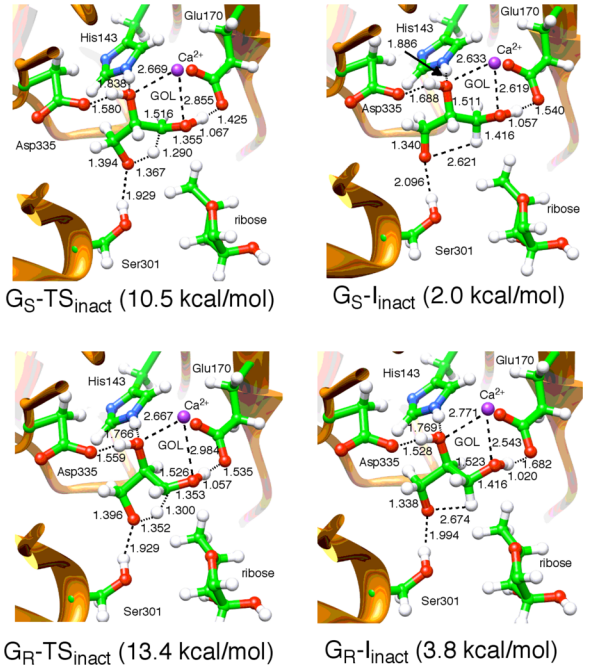

Figure 8. Optimized geometries of intermediate and transition states for inactivation in the G_S and G_R conformations (distances in angstroms). Relative energies are measured from G_S-RC shown in Figure 3a.

structures of the transition state for the hydrogen transfer (TS_{inact}) and I_{inact}. The transition state has a five-membered ring; the C1−H and O3−H bond lengths are 1.290 (1.300) and 1.367 (1.352) Å in G_S-TS_{inact} (G_R-TS_{inact}), respectively. The QM/MM-computed activation barrier is 20.5 (20.1) kcal/mol in the G_S (G_R) conformation measured from G_S-I1 (G_R-I1). This result indicates that the activation barrier height is not sensitive to the substrate-binding conformation. The relative energy of I_{inact} was calculated to be 2.0 (3.8) kcal/mol in G_S-I_{inact} (G_R-I_{inact}). The O-centered radical is unstable and is easily decomposed to formaldehyde and glycol radical by homolytic cleavage of the C2−C3 bond. The activation barrier of the decomposition is calculated to be 5.8 kcal/mol in the G_S conformation. The produced formaldehyde molecule is likely to

Scheme 1. Possible Inactivation Pathway

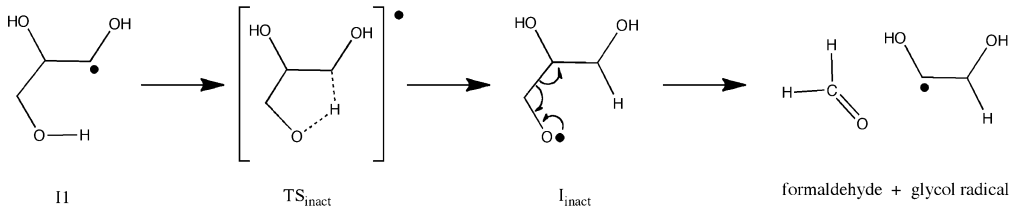

dx.doi.org/10.1021/bi300488u | Biochemistry 2012, 51, 9202−9210

react with the divalent cobalt of cobalamin and the glycol radical, forming an inactive cobalamin like formylcobalamin. Actually, an alkylcobalamin-like spectrum is observed upon glycerol inactivation,[27] although it is gradually changed to a hydroxocobalamin-like one by dialysis.[35] Formylcobalamin, whose spectrum is similar to that of alkylcobalamin, was unstable and slowly decomposed to hydroxocobalamin.

Figure 9 depicts the energy difference between TS_{inact} and TS2 in the G_S and G_R conformations. The activation barrier for

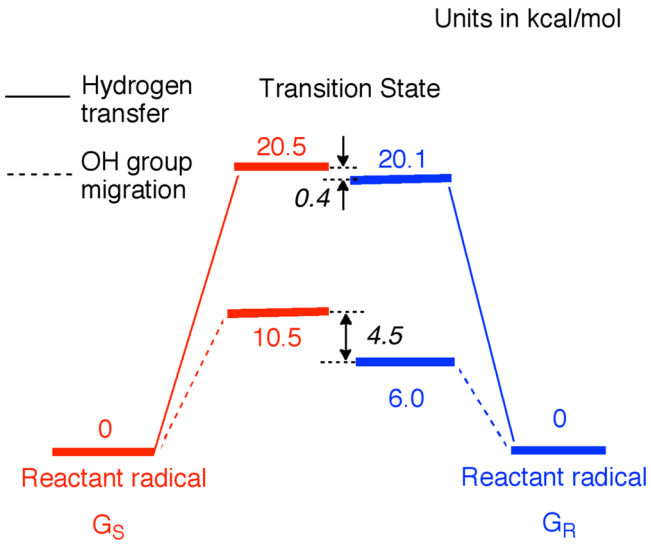

Figure 9. Activation barriers of OH group migration and hydrogen transfer in the G_S (red) and G_R (blue) conformations (units of kilocalories per mole).

TS_{inact} does not depend on the substrate-binding conformation. On the other hand, the activation energy of TS2, which is in a competitive reaction with TS_{inact}, significantly depends on the conformation (10.5 kcal/mol for G_S and 6.0 kcal/mol for G_R). The barrier differences between TS_{inact} and TS2 are 10.0 and 14.1 kcal/mol in the G_S and G_R conformations, respectively. It seems reasonable that the inactivation mainly proceeds in the G_S conformation because of the small energy difference. Moreover, G_S-I1 is favorable for the inactivation because of the shorter distance between C1 and 3-OH in I1. The C1−H (3-OH) distances are calculated to be 3.185 and 2.659 Å for G_R-I1 and G_S-I1, respectively. The hydrogen transfer is energetically and structurally inhibited in G_R-I1 to suppress the undesired inactivation reaction.

CONCLUSIONS

We have studied the product-forming and inactivation mechanism of diol dehydratase in the glycerol dehydration reaction using QM/MM calculations. The inactivation proceeds as follows. A hydrogen atom is transferred from the 3-OH group of glycerol to the C1 radical in the reactant radical intermediate to produce an O-centered radical, and then, the O-centered radical is decomposed to formaldehyde and glycol radical. Calculated activation barriers do not depend on the substrate-binding conformation. On the other hand, the activation barrier for OH group migration, which is a competitive reaction with hydrogen transfer, is significantly changed by the difference in the conformation. The activation barrier is 4.5 kcal/mol lower in the G_R conformation than in the G_S conformation. Our calculations suggest that Glu170 plays a critical role in stabilizing the reactant radical in the G_S conformation. Moreover, the hydrogen bonding interaction between Ser301 and the 3-OH group of glycerol lowers the activation barrier in G_R-TS2. As a result, we obtained an energy difference of 10.0 kcal/mol between the transition states for the hydrogen transfer and OH group migration in the G_S conformation, which is 4.1 kcal/mol smaller than that in the G_R conformation. These results indicate that enzyme inactivation is likely to proceed in the G_S conformation, which is consistent with the results of deuterioglycerol reactions.

ASSOCIATED CONTENT

Supporting Information

Energy diagram, one table of energies, one table of bond orders, one table of energy decomposition, and *XYZ* coordinates of the optimized structures. This material is available free of charge via the Internet at http://pubs.acs.org.

AUTHOR INFORMATION

Corresponding Author

*Institute for Materials Chemistry and Engineering and International Research Center for Molecular Systems, Kyushu University, Fukuoka 819-0395, Japan. Phone: +81-92-802-2529. E-mail: kazunari@ms.ifoc.kyushu-u.ac.jp.

Funding

K.Y. acknowledges Grants-in-Aid (22245028 and 24109014) for Scientific Research from JSPS and the Ministry of Culture, Sports, Science and Technology of Japan (MEXT), the Nanotechnology Support Project, the Nanotechnology Support Project of MEXT, the MEXT Project of Integrated Research on Chemical Synthesis, the MEXT program "Elements Strategy Initiative to Form Core Research Center" (since 2012), and CREST of Japan Science and Technology Corp. for their support of this work. T.T. also acknowledges Grants-in-Aid for Scientific Research [(B) 17370038 and (C) 22570143] from JSPS and MEXT and a Grant in Aid for Natural Sciences Research from the Asahi Glass Foundation (Tokyo, Japan).

Notes

The authors declare no competing financial interest.

ABBREVIATIONS

DD, diol dehydratase; AdoCbl, adenosylcobalamin; PDO, 1,2-propanediol; GOL, glycerol; QM, quantum mechanical; MM, molecular mechanical; G_S, glycerol bound to the enzyme with the *pro-S*-CH_2OH group at the site involved in hydrogen abstraction; G_R, glycerol bound to the enzyme with the *pro-R*-CH_2OH group at the site involved in hydrogen abstraction; PDB, Protein Data Bank; MD, molecular dynamics; ABNR, adopted basis Newton−Raphson; RC, reactant complex; TS1, transition state 1 (hydrogen abstraction); I1, intermediate 1 (reactant radical); TS2, transition state 2 (OH group migration); I2, intermediate 2 (product radical); TS3, transition state 3 (hydrogen recombination); I3, intermediate 3 (1,1,3-propanetriol); TS_{inact}, transition state for the side reaction; I_{inact}, intermediate for the side reaction (O-centered radical).

REFERENCES

(1) Dolphin, D., Ed. (1982) *B12*, John Wiley & Sons, New York.
(2) Banerjee, R., Ed. (1999) *Chemistry and biochemistry of B12*, John Wiley & Sons, New York.

(3) Toraya, T. (2003) Radical catalysis in coenzyme B_{12}-dependent isomerization (eliminating) reactions. *Chem. Rev. 103*, 2095−2127.
(4) Toraya, T. (2000) Radical catalysis of B_{12} enzymes: Structure, mechanism, inactivation, and reactivation of diol and glycerol dehydratases. *Cell. Mol. Life Sci. 57*, 106−127.
(5) Zagalak, B., Frey, P. A., Karabatsos, G. L., and Abeles, R. H. (1966) The stereochemistry of the conversion of D and L 1,2-propanediols to propionaldehyde. *J. Biol. Chem. 241*, 3028−3035.
(6) Frey, P. A., Essenberg, M. K., and Abeles, R. H. (1967) Studies on the mechanism of hydrogen transfer in the cobamide coenzyme-dependent dioldehydrase reaction. *J. Biol. Chem. 242*, 5369−5377.
(7) Frey, P. A., and Abeles, R. H. (1966) The role of the B_{12} coenzyme in the conversion of 1,2-propanediol to propionaldehyde. *J. Biol. Chem. 241*, 2732−2733.
(8) Frey, P. A., Kerwar, S. S., and Abeles, R. H. (1967) The participation of the two non-equivalent C-5′ hydrogens of B_{12}-coenzyme in the catalytic process. *Biochem. Biophys. Res. Commun. 29*, 873−874.
(9) Essenberg, M. K., Frey, P. A., and Abeles, R. H. (1971) Studies on the mechanism of hydrogen transfer in the coenzyme B_{12} dependent dioldehydrase reaction II. *J. Am. Chem. Soc. 93*, 1242−1251.
(10) Abeles, R. H., and Lee, H. A., Jr. (1964) Studies of the mechanism of action of cobamide coenzyme. *Ann. N.Y. Acad. Sci. 112*, 695−702.
(11) Rétey, J., Umani-Ronchi, A., Seibl, J., and Arigoni, D. (1966) Zum Mechanismus der Propandioldehydrase-Reaktion. *Experientia 22*, 502−503.
(12) Rétey, J., Umani-Ronchi, A., and Arigoni, D. (1966) Zur Stereochemie der Propandioldehydrase-Reaktion. *Experientia 22*, 72−73.
(13) Müller, P., and Rétey, J. (1983) A catalytic model for the dioldehydratase reaction. *J. Chem. Soc., Chem. Commun.*, 1342−1344.
(14) Rétey, J. (1990) Enzymic reaction selectivity by negative catalysis or how do enzymes deal with highly reactive intermediates. *Angew. Chem., Int. Ed. 29*, 355−361.
(15) Cockle, S. A., Hill, H. A. O., Williams, R. J. P., Davies, S. P., and Foster, M. A. (1972) The detection of intermediates during the conversion of propane-1,2-diol to propionaldehyde by glycerol dehydrase, a coenzyme B_{12} dependent reaction. *J. Am. Chem. Soc. 94*, 275−277.
(16) Finlay, T. H., Valinsky, J., Mildvan, A. S., and Abeles, R. H. (1974) Electron spin resonance studies with dioldehydrase. Evidence for radical intermediates in reactions catalyzed by coenzyme B_{12}. *J. Biol. Chem. 248*, 1285−1290.
(17) Valinsky, J. E., Abeles, R. H., and Fee, J. A. (1974) Electron spin resonance studies on diol dehydrase. 3. Rapid kinetic studies on the rate of formation of radicals in the reaction with propanediol. *J. Am. Chem. Soc. 96*, 4709−4710.
(18) Brown, K. L. (2005) Chemistry and Enzymology of Vitamin B_{12}. *Chem. Rev. 105*, 2075−2150.
(19) Shibata, N., Masuda, J., Tobimatsu, T., Toraya, T., Suto, K., Morimoto, Y., and Yasuoka, N. (1999) A new mode of B_{12} binding and the direct participation of a potassium ion in enzyme catalysis: X-ray structure of diol dehydratase. *Structure 7*, 997−1008.
(20) Masuda, J., Shibata, N., Morimoto, Y., Toraya, T., and Yasuoka, N. (2000) How a protein generates a catalytic radical from coenzyme B_{12}: X-ray structure of a diol-dehydratese-adeninylpentylcobalamin complex. *Structure 8*, 775−788.
(21) Shibata, N., Masuda, J., Morimoto, Y., Yasuoka, N., and Toraya, T. (2002) Substrate-induced conformational change of a coenzyme B12-dependent enzyme: Crystal structure of the substrate-free form of diol dehydratase. *Biochemistry 41*, 12607−12617.
(22) Shibata, N., Nakanishi, Y., Fukuoka, M., Yamanishi, M., Yasuoka, N., and Toraya, T. (2003) Structural rationalization for the lack of stereospecificity in coenzyme B_{12}-dependent diol dehydratase. *J. Biol. Chem. 278*, 22717−22725.
(23) Kamachi, T., Takahata, M., Toraya, T., and Yoshizawa, K. (2009) What is the identity of the metal ions in the active sites of coenzyme B_{12}-dependent diol dehydratase? A computational mutation analysis. *J. Phys. Chem. B 113*, 8435−8438.
(24) Toraya, T., Honda, S., and Mori, K. (2010) Coenzyme B12-dependent diol dehydratase is a potassium ion-requiring calcium metalloenzyme: Evidence that the substrate-coordinated metal ion is calcium. *Biochemistry 49*, 7210−7217.
(25) Kamachi, T., Doitomi, K., Takahata, T., Toraya, T., and Yoshizawa, K. (2011) Catalytic roles of the metal ion in the substrate-binding site of coenzyme B_{12}-dependent diol dehydratase. *Inorg. Chem. 50*, 2944−2952.
(26) Toraya, T., Shirakashi, T., Kosuga, T., and Fukui, S. (1976) Substrate specificity of coenzyme B_{12}-dependent diol dehydrase: Glycerol as both a good substrate and a potent inactivator. *Biochem. Biophys. Res. Commun. 69*, 475−480.
(27) Bachovchin, W. W., Eagar, J. R. G., Moore, K. W., and Richards, J. H. (1977) Mechanism of action of adenosylcobalamin: Glycerol and other substrate analogues as substrates and inactivators for propanediol dehydratase—Kinetics, stereospecificity, and mechanism. *Biochemistry 16*, 1082−1092.
(28) Bachovchin, W. W., Moore, K. W., and Richards, J. H. (1978) Mechanism of Action of Adenosylcobalamin: Hydrogen transfer in the inactivation of diol dehydratase by glycerol. *Biochemistry 17*, 2218−2224.
(29) Wagner, O. W., Lee, H. A., Frey, P. A., and Abeles, R. H. (1966) Studies on the mechanism of action of cobamide coenzymes. Chemical properties of the enzyme-coenzyme complex. *J. Biol. Chem. 249*, 1751−1762.
(30) Finlay, T. H., Valinsky, J., Sato, K., and Abeles, R. H. (1972) Studies on the mechanism of action of coenzyme B_{12}. The formation of 5′-deoxyadenosine and B_{12} (r) in the reaction of dioldehydrase with chloroacetaldehyde. *J. Biol. Chem. 247*, 4197−4207.
(31) Abend, A., Bandarian, V., Reed, G. H., and Frey, P. A. (2000) Identification of cis-ethanesemidione as the organic radical derived from glycolaldehyde in the suicide inactivation of dioldehydrase and of ethanolamine ammonia-lyase. *Biochemistry 39*, 6250−6257.
(32) Schwartz, P., LoBrutto, R., Reed, G. H., and Frey, P. A. (2003) Suicide Inactivation of Dioldehydrase by 2-Chloroacetaldehyde: Formation of the 'cis-Ethanesemidione' Radical, and the Role of a Monovalent Cation. *Helv. Chim. Acta 86*, 3764−3775.
(33) Sandala, G. M., Smith, D. M., Coote, M. L., and Radom, L. (2004) Suicide inactivation of dioldehydratase by glycolaldehyde and chloroacetaldehyde: An examination of the reaction mechanism. *J. Am. Chem. Soc. 126*, 12206−12207.
(34) Sandala, G. M., Smith, D. M., Coote, M. L., Golding, B. T., and Radom, L. (2006) Insights into the hydrogen-abstraction reactions of diol dehydratase: Relevance to the catalytic mechanism and suicide inactivation. *J. Am. Chem. Soc. 128*, 3433−3444.
(35) Yamanishi, M., Kinoshita, K., Fukuoka, M., Saito, T., Tanokuchi, A., Ikeda, Y., Obayashi, H., Mori, K., Shibata, N., Tobimatsu, T., and Toraya, T. (2012) Redesign of coenzyme B_{12} dependent diol dehydratase to be resistant to the mechanism-based inactivation by glycerol and act on longer chain 1,2-diols. *FEBS J. 279*, 793−804.
(36) Bashford, D., and Karplus, M. (1991) Multiple-site titration curves of proteins: An analysis of exact and approximate methods for their calculation. *J. Phys. Chem. 95*, 9556−9561.
(37) Dominy, B. N., and Brooks, C. L., III (1999) Development of a Generalized Born Model Parametrization for Proteins and Nucleic Acids. *J. Phys. Chem. B 103*, 3765−3773.
(38) Spassov, V. Z., and Yan, L. (2008) A fast and accurate computational approach to protein ionization. *Protein Sci. 17*, 1955−1970.
(39) Li, H., Robertson, A. D., and Jensen, J. H. (2005) Very fast empirical prediction and rationalization of protein pK_a values. *Proteins 61*, 704−721.
(40) Bas, D. C., Rogers, D. M., and Jensen, J. H. (2008) Very fast prediction and rationalization of pK_a values for protein−ligand complexes. *Proteins 73*, 765−783.

(41) Momany, F. A., and Rone, R. (1992) Validation of the General Purpose QUANTA3.2/CHARMm Force Field. *J. Comput. Chem. 13*, 888−900.
(42) Momany, F. A., Rone, R., Kunz, H., Frey, R. F., Newton, S. Q., and Schäfer, L. (1993) Geometry optimization, energetics and solvation studies on four- and five-membered cyclic and disulfide-bridged peptides, using the programs quanta3.3 and charmm22. *THEOCHEM 286*, 1−18.
(43) Brooks, B. R., Bruccoleri, R. E., Olafson, B. D., States, D. J., Swaminathan, S., and Karplus, M. (1983) CHARMM: A program for macromolecular energy, minimization, and dynamics calculations. *J. Comput. Chem. 4*, 187−217.
(44) Ryckaert, J.-P., Ciccotti, G., and Berendsen, H. J. C. (1977) Numerical integration of the Cartesian equations of motion of a system with constraints: Molecular dynamics of *n*-alkanes. *J. Comput. Phys. 23*, 327−341.
(45) Press, W. H., Flannery, B. P., Teukolshy, S. A., and Vetrrling, W. T. (1987) *Numerical Recipes: The Art of Scientific Computing*, University Press, Cambridge, U.K.
(46) Discovery Studio, version 2.0, Accelrys Software Inc., San Diego.
(47) ChemShell, http://www.chemshell.org (accessed December 10, 2007).
(48) Ahlrichs, R., Bär, M., Häser, M., Horn, H., and Kölmel, C. (1989) Electronic structure calculations on workstation computers: The program system turbomole. *Chem. Phys. Lett. 162*, 165−169.
(49) Smith, W., and Forester, T. R. (1996) DL_POLY_2.0: A general-purpose parallel molecular dynamics simulation package. *J. Mol. Graphics 14*, 136−141.
(50) Antes, I., and Thiel, W. (1998) On the treatment of link atoms in hybrid methods. In *Hybrid Quantum Mechanical and Molecular Mechanical Methods* (Gao, J., Ed.) pp 50−65, American Chemical Society, Washington, DC.
(51) Becke, A. D. (1988) Density-functional exchange-energy approximation with correct asymptotic behavior. *Phys. Rev. A 38*, 3098−3100.
(52) Becke, A. D. (1993) Density-functional thermochemistry. III. The role of exact exchange. *J. Chem. Phys. 98*, 5648−5652.
(53) Lee, C., Yang, W., and Parr, R. G. (1988) Development of the Colle-Salvetti correlation-energy formula into a functional of the electron density. *Phys. Rev. B 37*, 785−789.
(54) Schäfer, A., Horn, H., and Ahlrichs, R. (1992) Fully optimized contracted Gaussian basis sets for atoms Li to Kr. *J. Chem. Phys. 97*, 2571−2577.
(55) Schäfer, A., Huber, C., and Ahlrichs, R. (1994) Fully optimized contracted Gaussian basis sets of triple zeta valence quality for atoms Li to Kr. *J. Chem. Phys. 100*, 5829−5835.
(56) Bakowies, D., and Thiel, W. (1996) Hybrid Models for Combined Quantum Mechanical and Molecular Mechanical Approaches. *J. Phys. Chem. 100*, 10580−10594.
(57) Buckel, W., Kratky, C., and Golding, B. T. (2006) Stabilisation of Methylene Radicals by Cob(II)alamin in Coenzyme B_{12} Dependent Mutases. *Chem.—Eur. J. 12*, 352−362.
(58) Billeter, S. R., Turner, A. J., and Thiel, W. (2000) Linear scaling geometry optimization and transition state search in hybrid delocalised internal coordinates. *Phys. Chem. Chem. Phys. 2*, 2177−2186.
(59) Buley, A. L., Norman, R. O. C., and Pritchett, R. T. (1966) Stabilisation of Methylene Radicals by Cob(II)alamin in Coenzyme B_{12} Dependent Mutases. *J. Chem. Soc. B 1966*, 849−852.
(60) Gilbert, B. C., Larkin, J. P., and Norman, R. O. C. (1972) Electron spin resonance studies. Part XXXIII. Evidence for heterolytic and homolytic transformations of radicals from 1,2-diols and related compounds. *J. Chem. Soc., Perkin Trans. 2*, 794−802.
(61) Hayon, E., and Simic, M. (1974) Acid-base properties of free radicals in solution. *Acc. Chem. Res. 7*, 114−121.
(62) Golding, B. T., and Radom, L. (1973) Facilitation of intramolecular 1,2-shifts in radicals by protonation, and the mechanism of reactions catalysed by 5′-deoxyadenosylcobalamin. *J. Chem. Soc., Chem. Commun.*, 939−941.
(63) Golding, B. T., and Radom, L. (1976) On the mechanism of action of adenosylcobalamin. *J. Am. Chem. Soc. 98*, 6331−6338.
(64) Smith, D. M., Golding, B. T., and Radom, L. (1999) Toward a consistent mechanism for diol dehydratase catalyzed reactions: An application of the partial-proton-transfer concept. *J. Am. Chem. Soc. 121*, 5700−5704.
(65) Smith, D. M., Golding, B. T., and Radom, L. (2001) Understanding the mechanism of B_{12}-dependent diol dehydratase: A synergistic retro-push-pull proposal. *J. Am. Chem. Soc. 123*, 1664−1675.
(66) Sandala, G. M., Smith, D. M., and Radom., L. (2010) Modeling the reactions catalyzed by coenzyme B_{12}-dependent enzymes. *Acc. Chem. Res. 43*, 642−651.
(67) Kamachi, T., Toraya, T., and Yoshizawa, K. (2004) Catalytic roles of active-site amino acid residues of coenzyme B_{12}-dependent diol dehydratase: Protonation state of histidine and pull effect of glutamate. *J. Am. Chem. Soc. 126*, 16207−16216.
(68) Kamachi, T., Toraya, T., and Yoshizawa, K. (2007) Computational mutation analysis of hydrogen abstraction and radical rearrangement steps in the catalysis of coenzyme B_{12}-dependent diol dehydratase. *Chem.—Eur. J. 13*, 7864−7873.
(69) We also calculated models in which the three residues are included in the QM region to check the sensitivity of the data. The activation barrier of G_S-TS2 (G_R-TS2) is only 0.7 (0.9) kcal/mol higher than the original one.
(70) We also performed single-point calculations with the large QM model in which Arg193, Ser202, Thr222, Thr259, and Arg348 are included in the QM region. The activation barrier of G_S-TS2 (G_R-TS2) is 12.6 (7.5) kcal/mol, which is only 0.2 (0.3) kcal/mol higher than the original one.
(71) Wetmore, S. D., Smith, D. M., and Radom, L. (2001) Catalysis by Mutants of Methylmalonyl-CoA Mutase: A Theoretical Rationalization for a Change in the Rate-Determining Step. *ChemBioChem 2*, 919−222.
(72) Bucher, D., Sandala, G. M., Durbeej, B., Radom, L., and Smith, D. M. (2012) The Elusive 5′-Deoxyadenosyl Radical in Coenzyme-B12-Mediated Reactions. *J. Am. Chem. Soc. 134*, 1591−1599.
(73) Sandala, G. M., Kovacevic, B., Baric, D., Smith, D. M., and Radom, L. (2009) On the Reaction of Glycerol Dehydratase with But-3-ene-1,2-diol. *Chem.—Eur. J. 15*, 4865−4873.